

# Mixed convection from semi-circular cylinder in Bingham plastic fluids: Adding buoyancy

Anjali Gupta<sup>a</sup>, Krutika Iyer Ganesh<sup>a</sup>, Roderick Melnik<sup>b,c</sup>, Anurag Kumar Tiwari<sup>a,\*</sup>

<sup>a</sup>Department of Chemical Engineering, National Institute of Technology, Jalandhar 144011, Punjab, India

<sup>b</sup>Wilfrid Laurier University, 75 University Avenue West, Waterloo, ON N2L 3C5, Canada

<sup>c</sup>BCAM Basque Center for Applied Mathematics, Mazarredo Zumarkalea, 14, 48009 Bilbo, Bizkaia, Spain

## ARTICLE INFO

### Article history:

Available online 10 February 2022

### Keywords:

Rheology  
Semi-circular cylinder  
Bingham plastic fluids  
Nusselt number  
Richardson number  
Non-Newtonian fluids

## ABSTRACT

Mixed convection heat transfer from a heated semi-circular cylinder in Bingham plastic fluids with adding buoyancy configuration has been studied numerically. Extensive results of fluid flow and heat transfer characteristics are presented in terms of the velocity and temperature profiles, shape and size of yield/unyielded zone. In the steady flow regime, Reynolds number, Prandtl number, and Richardson number are expected to be positively dependent on the average Nusselt number (which decreases the convection boundary layer). In contrast, the average Nusselt number decreases as the value of the Bingham number increases from its maximum value in Newtonian media to its conduction limit when most of the fluid is frozen. Finally, using a simple expression, the numerical results of average Nusselt number have been predicted in terms of the  $j$ -factor for new applications.

Copyright © 2022 Elsevier Ltd. All rights reserved.

Selection and peer-review under responsibility of the scientific committee of the International Chemical Engineering Conference 2021 (100 Glorious Years of Chemical Engineering & Technology).

## 1. Introduction

Since non-Newtonian fluid behavior occurs frequently in a wide range of chemical process industries (e.g., polymers, pharmaceutical and food products, and health-care products), a considerable amount of research and practical activity has been devoted to determining the effect of non-Newtonian fluid rheology on hydrodynamics and heat transfer characteristics for various geometries [1,2]. A cursory review of the available studies on Newtonian flow and heat transfer past an unconfined circular cylinder reveals that most conditions of interest are now adequately represented. The corresponding flow of Bingham plastic fluids around a circular cylinder, on the other hand, has received very little attention. For instance, Mitsoulis [3] carried out a study of the wall effects on the creeping flow ( $Re \rightarrow 0$ ) of Bingham fluids over a circular cylinder. At low Bingham numbers, they found the wall effects to be significant. This is due to the fact that when the Bingham number increases, fluid-like regions become close to the cylinder, and hence no wall effect is expected under such conditions. They also presented correlations for drag based on his numerical predictions.

The drag coefficient and flow kinematics were then given as functions of the Oldroyd number (or Bingham Number) by Tokpavi et al. [4], which used the Bingham constitutive equation with Papanastasiou's regularization approach. A detailed investigation on the shapes and locations of rigid zones was also presented. Both numerical and experimental investigations of the flow past a circular cylinder at finite Reynolds numbers have been critically examined by Mossaz et al. [5]. In terms of streamline and isotherm contours, yielded/unyielded regions, drag, and Nusselt number, Nirmalkar and Chhabra [6] presented detailed numerical results of forced convection. The Reynolds number, Bingham number, and Prandtl number all have a positive relationship with the Nusselt number. Due to the orientation of the bluff body, which is a significant additional parameter which determines the flow phenomena, one would not expect the flow to be similar to the flow over a semi-circular cylinder. Tiwari and Chhabra [7,8] have been analyzing the flow stream of Bingham plastic fluids over a heated semi-circular cylinder with its flat side facing the approaching flow for the past few years. Their findings apply to two convection regimes: free and forced, although they are all limited to the so-called steady flow regime. Following that, they presented some preliminary findings on hydrodynamic forces and heat transfer rate values in the laminar shedding regime. Bhinder et al [9] performed unsteady simulations for air as the operating fluid for var-

\* Corresponding author.

E-mail address: [tiwaria@nitj.ac.in](mailto:tiwaria@nitj.ac.in) (A. Kumar Tiwari).

ious values of the Reynolds number ( $80 \leq Re \leq 180$ ) and incidences angle ( $0 \leq \alpha \leq 180^\circ$ ). They observed that when the angle of incidence increases, the variation of the drag coefficient decreases. They also identified a relationship between the Strouhal and Nusselt numbers, as well as Reynolds number and angle of incidence. After that, Chatterjee et al. [10] conducted unsteady simulations for Reynolds number ranges with a fixed Prandtl number ( $Pr = 0.7$ ) for two alternative semi-circular cylinder configurations. They determined that when the velocity and temperature fields are orientated in the direction of the curved surface, rather than the flat surface, is unstable. From the preceding discussion, it is clear that only limited study is available on the forced convection heat transfer characteristics of a two-dimensional semi-circular cylinder even in Newtonian fluids, let alone in Bingham plastic fluids. This study aims to address this problem by studying the mixed convection of a semi-circular cylinder with a flat base pointed upstream, particularly in Bingham plastics fluids.

## 2. Problem description and governing equations

Let us consider a semi-circular cylinder of diameter  $D$  (infinitely long in the  $z$ -direction) at isothermal boundary condition ( $T_w$ ) which is kept in a uniform stream of a Bingham plastic fluid with velocity,  $U$  and temperature,  $T_\infty < T_w$  (Fig. 1a). The rate of heat transfer from the isothermal semi-circular cylinder to the fluid occurs in the adding buoyancy configuration where both imposed and buoyancy-induced flows are directed in the same direction.

This semi-circular cylinder is enclosed by an artificial circular envelope of fluid (diameter approximates  $D_\infty$ ) for this unconfined flow condition (Fig. 1). Incompressible fluids, two-dimensional, steady and laminar flow, neglected viscous dissipation terms and Boussinesq approximation are made as simplified assumptions in this work. Under the small temperature difference, neglected the temperature dependence thermo-physical properties with temperature (except density term in  $y$ -momentum Eq). In the study flow regimes, governing differential equations (written in their dimensionless forms) are as follows [11]:

$$\text{Continuity equation } \nabla \cdot \mathbf{U} = 0 \quad (1)$$

$$\text{Momentum equation : } (\mathbf{U} \cdot \nabla) \mathbf{U} = -\nabla p + \frac{1}{Re} (\nabla \cdot \boldsymbol{\tau}) + Ri\theta\delta_{iy} \quad (2)$$

$$\text{Energy Equation : } (\mathbf{U} \cdot \nabla)\theta = \frac{1}{Re \times Pr} (\nabla^2 \theta) \quad (3)$$

The dimensional variables in governing equations (1–3) are non-dimensionalized using the scaling variables,

$$x = \frac{X'}{D}, y = \frac{Y'}{D}, U_x = \frac{U'_x}{U_\infty}, U_y = \frac{U'_y}{U_\infty}, p = \frac{p'}{\rho U_\infty^2}, \tau = \frac{\tau'}{(\mu_B \frac{U_\infty}{D})}, \theta = \frac{(T - T_\infty)}{(T_w - T_\infty)}$$

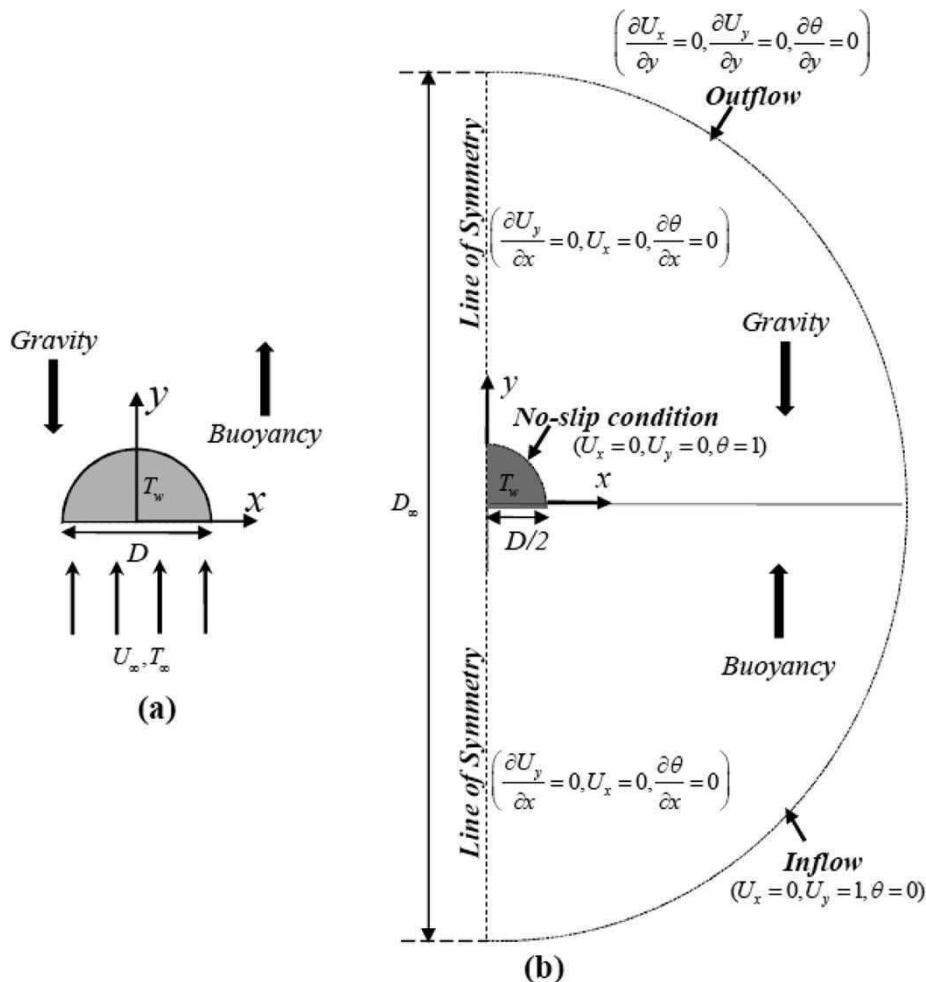


Fig. 1. Schematics of the unconfined flow over a semi-circular cylinder: (a) Physical model (b) Computational domain.

In this problem, the flow is assumed to be laminar, steady, symmetric about the  $y$ -axis and two-dimensional for the range of conditions spanned here. For incompressible fluids, the extra stress tensor is written as,  $\tau = 2\mu\dot{\gamma}$  where  $\dot{\gamma}$  is the rate of deformation tensor which can be written as,  $\dot{\gamma} = 1/2(\nabla U + \nabla U^T)$ . For a Bingham plastic fluid model, the rheological constitutive equation (dimensionless) for simple shear flow is defined as:

$$\tau = \left(1 + \frac{Bn}{|\dot{\gamma}|}\right)\dot{\gamma}, \text{ if } |\tau| > Bn \quad (4a)$$

$$\dot{\gamma} = 0, \text{ if } |\tau| \leq Bn \quad (4b)$$

Owing to its discontinuous behaviour of Eq. (4). It is difficult to incorporate it directly in governing Eq. (2) and solve it numerically. To overcome this problem, Papanastasiou regularization models [12] is used to provide a smooth transition between yielded and unyielded region with growth rate parameter,  $m$  which is defined as,

$$\eta = 1 + \frac{Bn \left\{ 1 + \exp(-m\sqrt{\text{tr}(\dot{\gamma}^2)}) \right\}}{\sqrt{\text{tr}(\dot{\gamma}^2)}} \quad (5)$$

Finally, it is required for physically boundary conditions for this configuration have to be applied at the inlet boundary ( $U_x = 0, U_y = 1, \theta = 0$ ), on the cylinder surface ( $U_x = 0, U_y = 0, \theta = 1$ ), the exit boundary,  $\partial\varphi/\partial x = 0$ , (where  $\varphi$  is  $U_x, U_y$  and  $\theta$ ), and the plane of symmetry ( $U_x = 0, \partial U_y/\partial x = 0, \partial\theta/\partial x = 0$ ). The dimensionless groups appearing in the aforementioned governing equations are defined as follows:

$$\begin{aligned} \text{Bingham number } Bn &= \frac{\tau_0 D}{\mu_B U_\infty} \text{ Reynolds number, } Re \\ &= \frac{\rho U_\infty D}{\mu_B} \text{ Richardson number } Ri = \frac{Gr}{Re^2} \end{aligned} \quad (6)$$

For large values of this parameter  $Ri \rightarrow \infty$  indicate to the free convection regime whereas vanishingly small values  $Ri \rightarrow 0$  indicate the negligible influence of free convection. At  $Ri = 1$ , the external velocity and the buoyancy-induced velocity are of comparable magnitudes. The numerical solution of the aforementioned governing equations subject to the above-noted boundary conditions maps the flow domain in terms of the primitive variables  $U_x, U_y, P$  and  $\theta$ . These, in turn, can be processed further to evaluate the derived parameters which characterize the momentum and heat transfer characteristics of the semi-circular cylinder.

$$\text{Nusselt number : } Nu = \frac{hD}{k} = -\frac{\partial\theta}{\partial n_s} \quad (7)$$

Where  $h$  is the local heat transfer coefficient and  $n_s$  the surface outward unit normal. On the other hand, gross engineering parameter average Nusselt number,  $Nu_{avg} = 1/S \int_S Nuds$  which is frequently used in process engineering applications. In the mixed convection regime, both fluid mechanics and heat transfer characteristics are influenced by dimensional considerations Reynolds number ( $Re$ ), Prandtl number ( $Pr$ ), Richardson number ( $Ri$ ) and Bingham number ( $Bn$ ). The main objective of this study is to explore and develop these relationships for the average Nusselt number.

### 3. Results and discussion

Mixed convection heat transfer in Bingham plastic fluids is studied for the following ranges of conditions: Richardson number

( $0 \leq Ri \leq 2$ ), Reynolds number ( $0.1 \leq Re \leq 30$ ), Prandtl number ( $10 \leq Pr \leq 100$ ) and Bingham number ( $0 \leq Bn \leq 10^3$ ) to elucidate their influences on the velocity and temperature fields as well as on the gross momentum and heat transfer characteristics.

#### 3.1. Numerical solution methodology and validations

In the present case, the finite element based solver COMSOL Multiphysics is used for solving the equations which map the flow domain in primitive variables  $U_x, U_y, p$  and  $\theta$ . The relative tolerance criteria of  $10^{-5}$  for the continuity, momentum and energy are used as convergence criteria for each case. In the present study, domain size ( $D_\infty/D=250$ ), grid size ( $\delta/D=0.0012$ ) and regularization parameter ( $m=10^6$ ) are used and sufficient for the present numerical investigation. Since no previous numerical results for the current configuration are available in the literature, equivalent results for a circular cylinder are used. The current and literature values of the local Nusselt number distribution across the surface of the cylinder in the mixed-convection regime in the air (Dennis and Chang [13]; Badr [14], Fig. 2). Based on the validation results along with our experience, the new results reported herein are considered to be reliable to within  $\sim 3$ –4% or so.

#### 3.2. Streamline and isotherm contours

The velocity and temperature fields near the semi-circular cylinder in terms of the streamline and isotherm contour are shown in Figs. 3 and 4 at different values of Bingham number ( $Bn$ ), Reynolds number ( $Re$ ), Prandtl number ( $Pr$ ) and Richardson number ( $Ri$ ). In the forced convection flow (i.e.,  $Ri = 0$ ), at small  $Re$  (such as  $Re = 0.1$ ), the fluid inertia is negligible and the flow remains attached to the surface of the semi-circular cylinder. Under these conditions, as the value of the  $Bn$  is progressively increased, the yielded zones diminish thereby sharpening the velocity and temperature gradients, as can be seen in Fig. 3. However, at high  $Re$  (such as at  $Re = 30$ ), under certain conditions, especially at low  $Bn$ , a well-developed recirculation zone develops in the rear side of the semi-circular cylinder. The size of the wake region decreases with increasing  $Bn$  until it vanishes entirely at  $Bn = 3$ , regardless of the value of the  $Ri$ . These findings suggest that

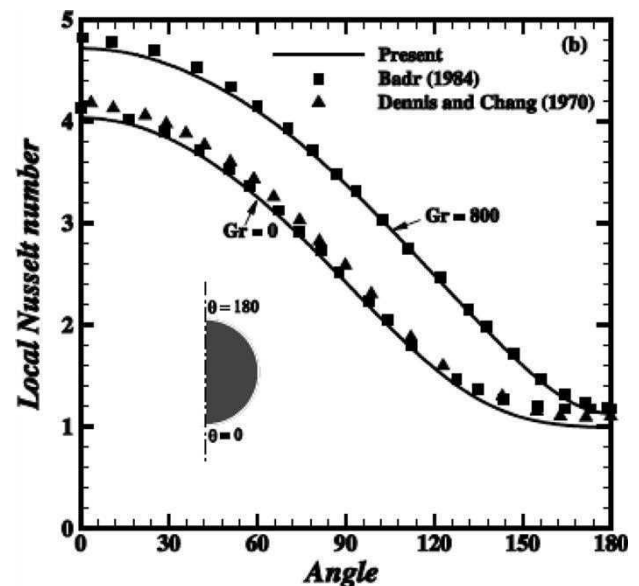


Fig. 2. Comparison between the present and literature results on local Nusselt number distribution on the surface of a circular cylinder at different values of  $Gr$  for the case of aiding buoyancy flow for  $Pr = 0.7$  and  $Re = 20$ .

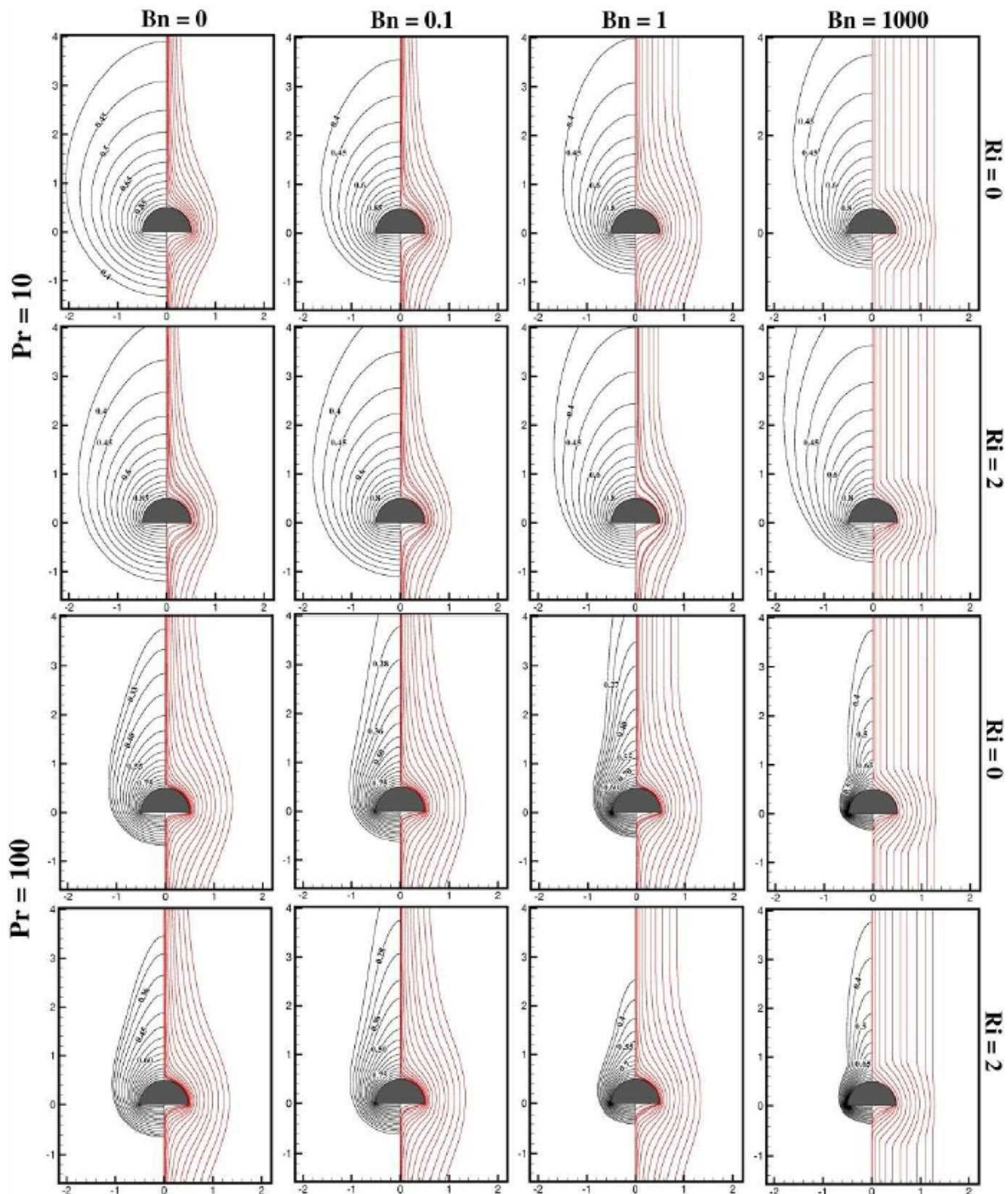


Fig. 3. Representative streamline (right-half) and isotherm (left-half) contours at  $Re = 0.1$ .

the  $Bn$  decreases the chance of the recirculation zone forming (Fig. 4). The  $Re$  values promote the formation of an unfavourable pressure gradient, which causes the flow to separate. However, for low  $Re$  ( $Re = 0.1$ ), the introduction of the buoyancy-induced flow appears to go hand-in-hand with the effect of the  $Re$ . On the other hand, the effect of the  $Ri$  is even more dramatic at high  $Re$  ( $Re = 30$ ), in so far that the rising plume also acts against the wake formation thereby shortening the recirculation region. Furthermore, at conduction dominant region (small value of  $Re$ ,  $Pr$  and/

or  $Ri$ ), the contours of the isotherm nearly resemble the shape of the semi-circular cylinder, as a result, the dominance of conduction is highlighted, although these profiles resemble streamline profiles, thereby denoting the enhanced role of the convection at high  $Re/Pr/Ri$ . The heat transfer is predicted to have a positive dependence on each of these parameters due to the thinning of the boundary layers as the values of  $Re$ ,  $Ri$ ,  $Pr$ , and  $Bn$  increase. The Nusselt number results presented in the subsequent sections support this conjecture.



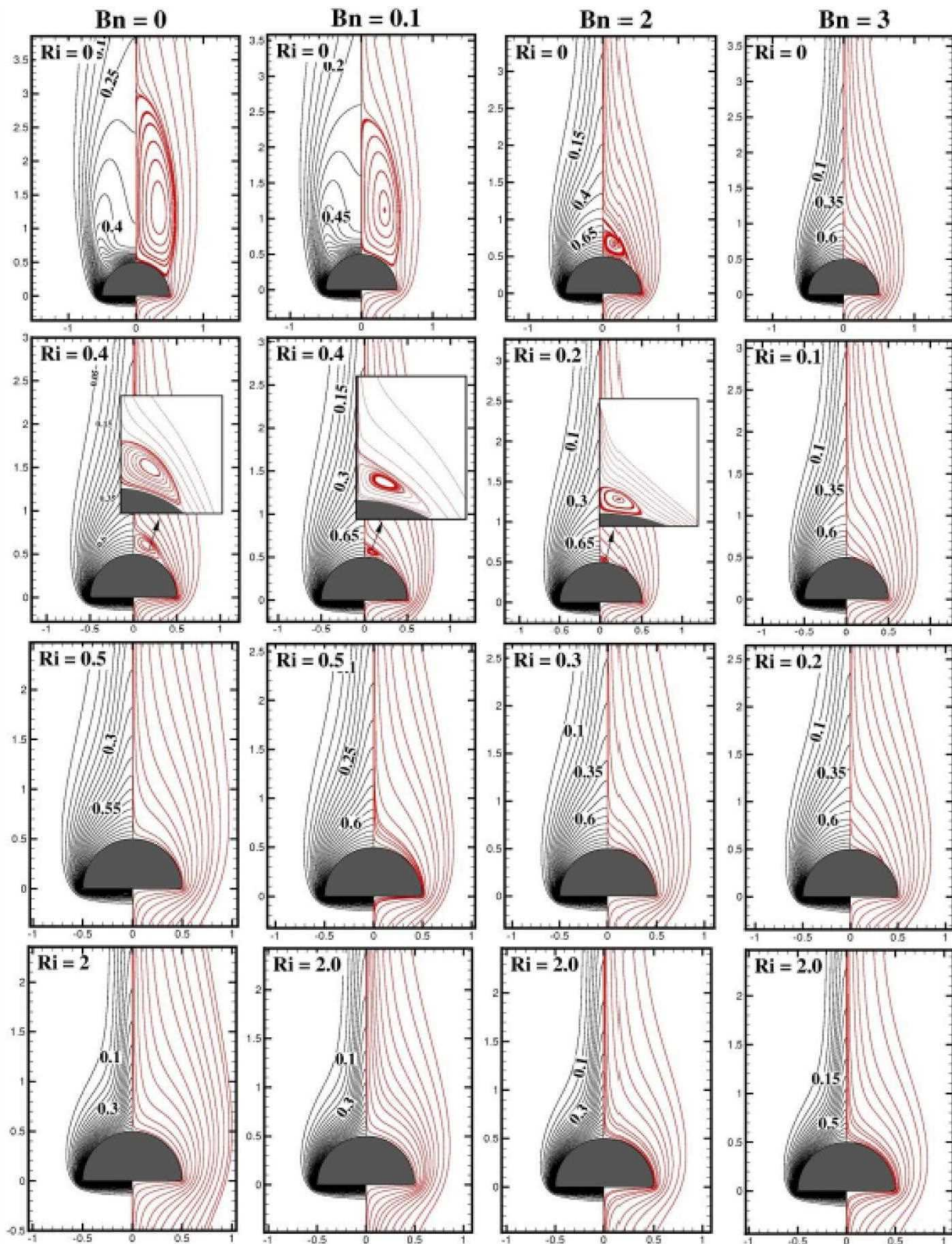


Fig. 4. Representative streamline (right-half) and isotherm (left-half) contours at  $Re = 30$  and  $Pr = 10$ .

### 3.3. Morphology of Yielded/Unyielded region

In the Bingham plastic fluids, depending on the magnitude of the stress level versus the value of the fluid yield stress, the flow domain is divided into yielded or fluid-like and unyielded or solid-like regions. To characterise the respective contributions of

conduction and convection heat transfer, it is typical to analyse the influence of  $Bn$ ,  $Re$ ,  $Pr$ , and  $Ri$  on the size and shape of the yielded/unyielded zones. Fig. 5(a)–(b) show representative plots of the yielded/unyielded regions at  $Re = 0.1$  and  $Re = 30$  for a variety of combinations of the  $Bn$ ,  $Pr$ , and  $Ri$ . It's important to remember that in the absence of buoyancy ( $Ri = 0$ ) and at low Reynolds

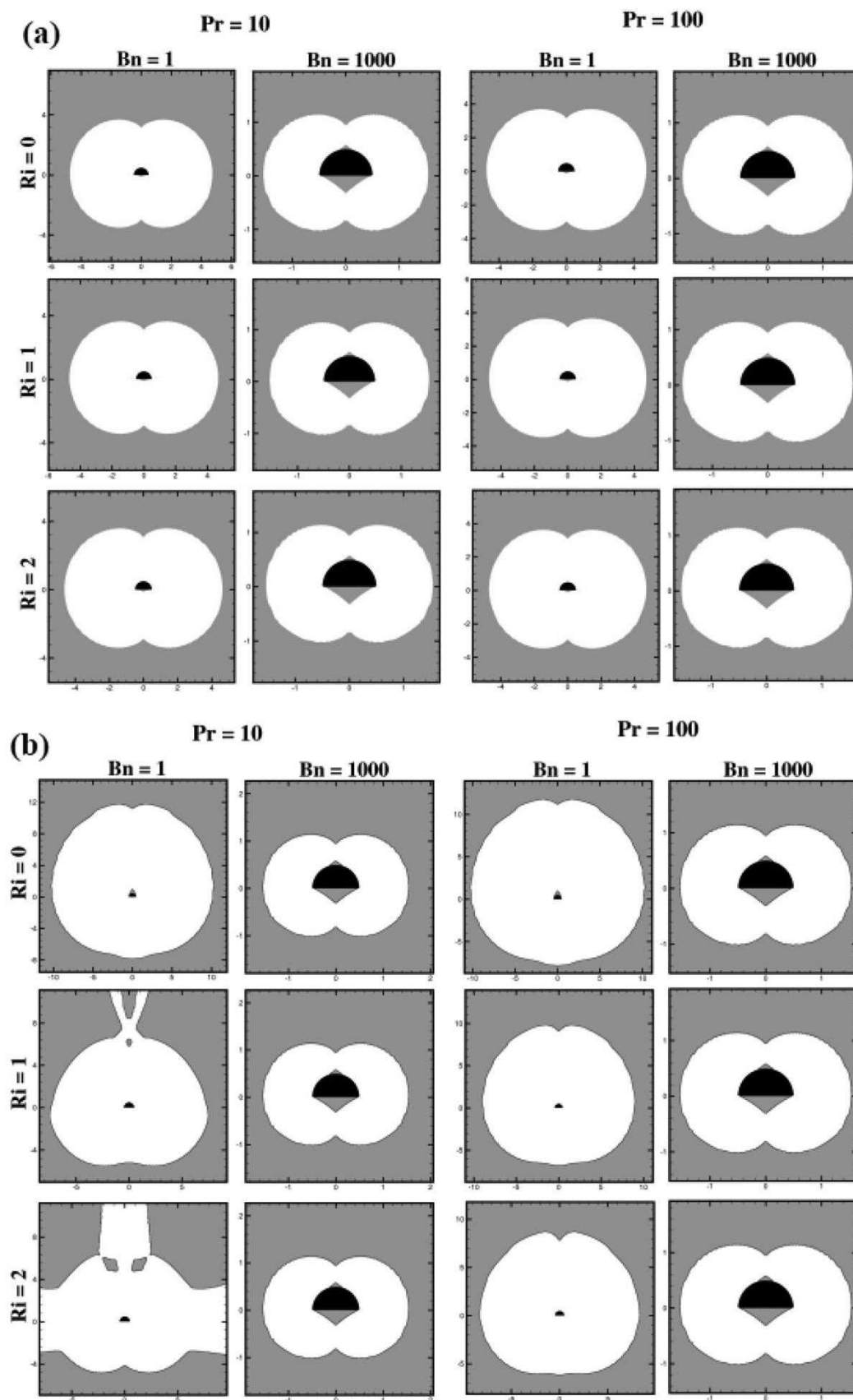


Fig. 5. Morphology of yielded/unyielded zones at (a)  $Re = 0.1$  and (b)  $Re = 30$ .

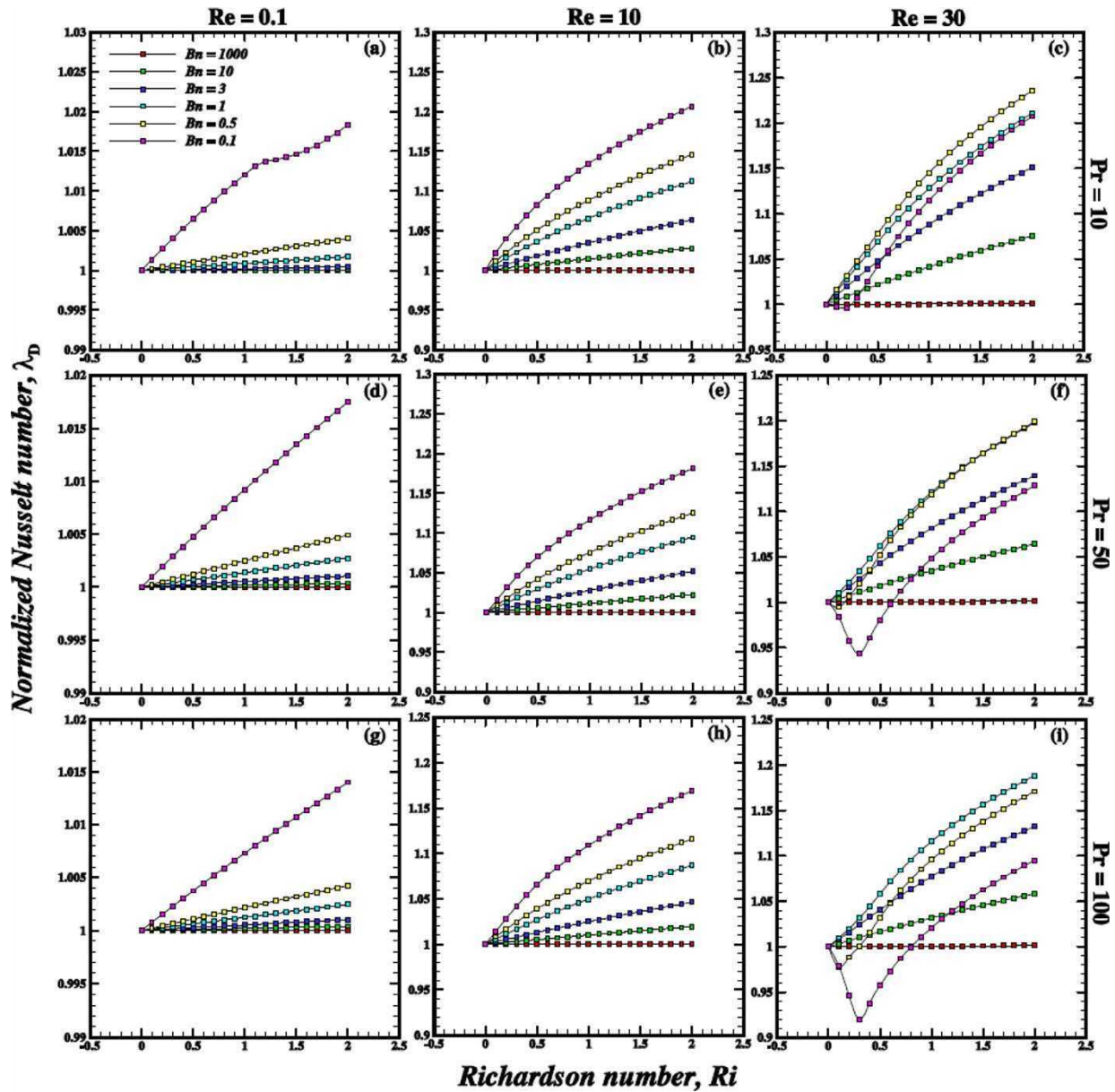


Fig. 6. Dependence of the normalized Nusselt number on the Ri, Bn, Pr and Re.

numbers ( $Re = 0.1$ ), there are two unyielded regions: a small amount of unyielded material adhering to the top and bottom (polar cap) of a semicircular cylinder that is static, and an outer envelope of unyielded fluid far away from the cylinder of fluid moving *en masse* with the free stream velocity. The stagnant zones are formed when the prevailing stress is not sufficient to overcome the yield stress of the fluids. These stagnant zones are called polar caps. It is observed that the polar caps at the rear of the semicircular cylinder are larger than those in the front of the semicircular cylinder. It can also be seen that the size of the yielded region decreases with the increasing  $Bn$  and expands with the increasing  $Re$  in the absence of the free convection effect as seen in Fig. 5(a). While for the buoyancy-induced flow, both the size and shape of the yielded region are observed to be slightly different as compared to that in the forced convection mode as seen in Fig. 5(b). Due to this new phenomenon, it is also observed that the size of the polar caps in the presence of buoyancy effect ( $Ri = 2$ ) was smaller than that in the absence of buoyancy effect ( $Ri = 0$ ). Altogether, it can be inferred that both free and forced convection favour the expansion of yielded regions while convection favours

the expansion of yielded regions while  $Bn$  tends to counter this tendency.

### 3.4. Average Nusselt number

The average Nusselt numbers ( $Nu_{avg}$ ) are frequently required in process engineering calculations from a practical standpoint. As a result, the surface averaged Nusselt number over the cylinder's surface has been reported in terms of normalised form (with forced convection)  $\lambda_D$ , which distinguishes the influence of free convection (Fig. 6). The  $Nu_{avg}$  value indicated a positive relationship with both  $Re$  and  $Pr$ , which is owing to temperature gradients' steeper slope over time. Furthermore, the normalized Nusselt number ( $\lambda_D$ ) also shows a positive dependence on  $Ri$  and inverse dependence on  $Bn$ . This is obviously due to the suppression of advection by the yield stress effects. As noted earlier, the  $Nu_{avg}$  can be represented by functional dependence,  $Nu_{avg} = f(Re, Pr, Bn, Ri)$ . The functional relationship can be simplified by introducing the effective velocity,  $U_{ch}$ , as was done by Bose et al. [15] simply as a sum of



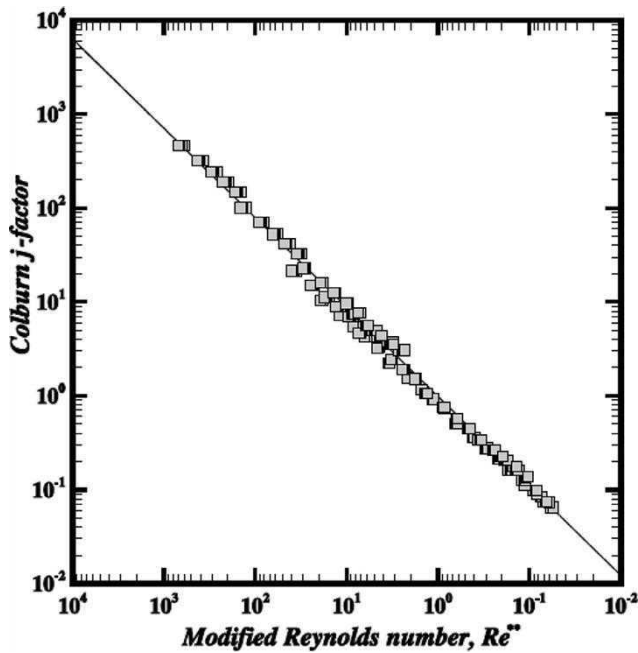


Fig. 7. Dependence of  $j$ -factor on the modified Reynolds number ( $Re^{**}$ ).

the external and buoyancy-induced contributions,  $U_{ch} = U_{\infty} + (g\beta D\Delta T)^{1/2}$ . This choice of velocity scaling yields the following definitions of the Reynolds number ( $Re^*$ ) and Bingham number ( $Bn^*$ ) and it also eliminates the Richardson number ( $Ri$ ) from the set of parameters,  $Re^* = Re(1 + \sqrt{Ri})$  and  $Bn^* = Bn/(1 + \sqrt{Ri})$ . Similarly, for Bingham plastic fluids, the effective fluid viscosity  $\mu_{eff} \cong \mu_B + \tau_0/\dot{\gamma}_c$  can be used as the viscosity scale instead  $\mu_B$ . This leads to further modifications in the definitions of the dimensionless groups as,  $Re^{**} = Re^*/(1 + Bn^*)$ ,  $Pr^* = Pr(1 + Bn^*)$ .

Thus, the functional relationship embodied can now be rewritten as follows,  $Nu_{avg} = f(Re^{**}, Pr^*)$ . This approach, however, still produces a set of curves that match the value of the modified Prandtl number,  $Pr^*$ . The data can be further consolidated by using the well-known Colburn  $j$ -factor, which is defined as:

$$j = \frac{Nu_{avg}}{Re^{**} Pr^{*1/3}} = f(Re^{**}) \quad (8)$$

The variation of the  $j$ -factor with the modified Reynolds number,  $Re^{**}$  are indicated in Fig. 7. Clearly, it shows the expected inverse dependence of the  $j$ -factor on  $Re^{**}$ . The following simple form is used to correlate the current numerical values ( $\sim 1260$  data points):

$$j = 1.2(Re^{**})^{-2/3} \quad (9)$$

Without any discernible trends, Eq. (9) reproduces the current numerical values with an average inaccuracy of 12.03 % that increases to a maximum of 26.14%. Furthermore, Eq.9 embodies the widely accepted scaling of the average Nusselt number ( $Nu_{avg} Pr^{*1/3}$  as well as that of  $j$ -factor  $j Re^{**2/3}$ ). It also contains the forced convection limiting case ( $Ri = 0$ ), in which  $Re^* = Re$  and  $Bn^* = Bn$ . It also takes into account the Newtonian limit, which is denoted by  $Bn = 0$ .

#### 4. Conclusions

Here, we deal with the flow and heat transfer characteristics for the aiding-buoyancy mixed convection heat transfer from a heated

semi-circular cylinder in the stream of Bingham plastic fluids has been investigated over the following ranges of conditions:  $0 \leq Ri \leq 2$ ,  $0 \leq Bn \leq 10^3$ ,  $0.1 \leq Re \leq 30$  and  $10 \leq Pr \leq 100$ . The detailed results on the flow and heat transfer characteristics are visualized in terms of the streamlines and isotherm contours near the surface of the cylinder. In general, increasing the  $Re$  and  $Pr$ , or both, tends to improve convection, and the size of the yielded zones shows a positive relationship with both parameters. Overall, with low value of  $Bn$ , the effect of forced convection is more pronounced. The value of  $Ri$  has a positive effect on the overall heat transfer when normalised with the corresponding forced convection values, although this dependence decreases with increasing value of  $Bn$ . Finally, the present numerical values of the  $Nu_{avg}$  have been correlated via the use of the  $j$ -factor.

#### Declaration of Competing Interest

The authors declare that they have no known competing financial interests or personal relationships that could have appeared to influence the work reported in this paper.

#### Acknowledgements

The authors are grateful to Dr. Neelkanth Nirmalkar, Assistant Professor, Department of Chemical engineering, Indian Institute of Technology Ropar India, for his continued support and for providing us with the computational facility.

#### References

- [1] R.P. Chhabra, J.F. Richardson, *Non-Newtonian Flow and Applied Rheology: Engineering Applications*, second ed., Butterworth-Heinemann, Oxford, 2008.
- [2] R.P. Chhabra, Fluid flow and heat transfer from circular and non-circular cylinders submerged in non-Newtonian liquids, *Adv. Heat Transfer* 43 (2011) 289–417, <https://doi.org/B978-0-12-381529-3.00004-9>.
- [3] E. Mitsoulis, On creeping drag flow of a viscoplastic fluid past a circular cylinder: wall effects, *Chem. Eng. Sci.* 59 (2004) 789–800, <https://doi.org/j.ces.2003.09.041>.
- [4] D.L. Tokpavi, A. Magnin, P. Jay, Very slow flow of Bingham viscoplastic flow around a circular cylinder, *J. Non-Newtonian Fluid Mech.* 154 (2008) 65–76, <https://doi.org/j.jnnfm.2008.02.006>.
- [5] S. Mossaz, P. Jay, A. Magnin, Criteria for the appearance of recirculating and non-stationary regimes behind a cylinder in a viscoplastic fluid, *J. Non-Newtonian Fluid Mech.* 165 (2010) 1525–1535, <https://doi.org/j.jnnfm.2010.08.001>.
- [6] N. Nirmalkar, R.P. Chhabra, Momentum and heat transfer from a heated circular cylinder in Bingham plastic fluids, *Int. J. Heat Mass Transfer* 70 (2014) 564–577, <https://doi.org/j.ijheatmasstransfer.2013.11.034>.
- [7] A.K. Tiwari, R.P. Chhabra, Free convection from a heated semi-circular cylinder in Bingham plastic fluids, *J. Thermophys. Heat Transfer* 30 (2016) 369–378, <https://doi.org/10.2514/1.T4688>.
- [8] A.K. Tiwari, R.P. Chhabra, Momentum and heat transfer from a semi-circular cylinder in Bingham plastic fluids, *Appl. Math. Model.* 39 (2015) 7045–7064, <https://doi.org/j.apm.2015.02.051>.
- [9] A.P.S. Bhinder, S. Sandip, A. Dalal, Flow over and forced convection heat transfer around a semi-circular cylinder at incidence, *Int. J. Heat Mass Transfer* 55 (2012) 5171–5184, <https://doi.org/j.ijheatmasstransfer.2012.05.018>.
- [10] D. Chatterjee, B. Mondal, P. Halder, Unsteady forced convection heat transfer over a semi-circular cylinder at low Reynolds numbers, *Numer. Heat Transfer; Part A: Appl.* 63 (2013) 411–429, <https://doi.org/10.1080/10407782.2013.742733>.
- [11] R.B. Bird, W.E. Stewart, E.N. Lightfoot, *Transport Phenomena*, second ed., Wiley, New York, 2002.
- [12] T.C. Papanastasiou, Flow of Materials with Yield, *J. Rheol.* 31 (1987) 385–404, <https://doi.org/10.1122/1.549926>.
- [13] S.C.R. Dennis, G.-Z. Chang, Numerical solutions for steady flow past a circular cylinder at Reynolds numbers up to 100, *J. Fluid Mech.* 42 (3) (1970) 471–489, <https://doi.org/10.1017/S0022112070001428>.
- [14] H.M. Badr, Laminar combined convection from a horizontal cylinder –parallel and contra flow regimes, *Int. J. Heat Mass Transfer* 27 (1) (1984) 15–27, [https://doi.org/10.1016/0017-9310\(84\)90233-3](https://doi.org/10.1016/0017-9310(84)90233-3).
- [15] A. Bose, N. Nirmalkar, R.P. Chhabra, Effect of aiding-buoyancy on mixed convection from a heated cylinder in Bingham plastic fluids, *J. Non-Newtonian Fluid Mech.* 220 (2015) 3–21, <https://doi.org/10.1016/j.jnnfm.2014.06.006>.